LAWRENCE
LIVERMORE
NATIONAL
LABORATORY

LLNL-CONF-707261

Results from Three Extreme Ultraviolet Spectrometers for Impurity Monitoring on NSTX-U

M. E. Weller, P. Beiersdorfer, V. A. Soukhanovskii, E. W. Magee, F. Scotti, M. L. Reinke

October 28, 2016

58th Annual Meeting of the APS Division of Plasma Physics
San Jose, CA, United States
October 31, 2016 through November 4, 2016

Results from Three Extreme Ultraviolet Spectrometers for Impurity Monitoring on NSTX-U

M.E. Weller, P. Beiersdorfer, V.A. Soukhanovskii, E.W. Magee,
F. Scotti, *LLNL,* M.L. Reinke, *ORNL,* PPPL Staff

58th Annual Meeting of the APS
Division of Plasma Physics
San Jose, CA, October 31 – November 4, 2016

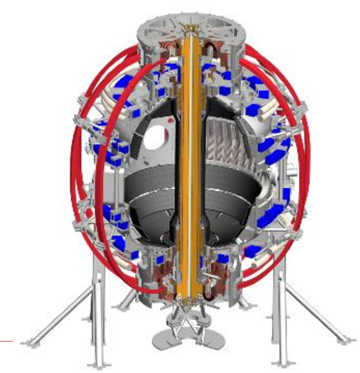

Abstract

The National Spherical Torus Experiment – Upgrade (NSTX-U) has been performing plasma operations for over a year and one of the focuses of study has been to monitor the levels of impurities emitting from plasma facing components (PFC). To monitor the levels of impurities three high resolution flat field grazing incident extreme ultraviolet (EUV) spectrometers capable of time resolution below 10 ms have been implemented on NSTX-U. The spectrometers are dubbed the X-ray and Extreme Ultraviolet Spectrometer (**XEUS**, 8 – 70 Å), the Metal Monitor and Lithium Spectrometer Assembly (**MonaLisa**, 50 – 220 Å), and the Long-Wavelength and Extreme Ultraviolet Spectrometer (**LoWEUS**, 190 – 440 Å). Confirmed lines measured by the spectrometers emit from He, Li, B, C, O, Ti, Cr, Fe, and Ni. Results of trends of various lines and line ratios measured are presented, including the Lyman-α (2p → 1s) transitions of O VIII at 18.9 Å, C VI at 33.7 Å, B V at 48.6 Å, Li III at 134.9 Å, and He II at 303.8 Å. Future plans include utilizing high-Z PFCs made of molybdenum and tungsten and also implementing a new laser blow-off (LBO) system.

This work was performed under the auspices of the US Department of Energy under DE-AC52-07NA27344 and DE-AC02- 09CH11466. LLNL-CONF-707261.

Brief History of EUV Spectroscopy on NSTX

- **XEUS** first introduced in 2004 on NSTX to study spectral line ratios useful as plasma diagnostics for astrophysics and for impurity monitoring with 50 ms time resolution (P. Beiersdorfer 2006).

- In 2007 **XEUS** was modified with a new detector which resulted in a time-resolution down to 25 ms (P. Beiersdorfer 2008).

- **LoWEUS** was added to NSTX in 2008 to cover longer wavelengths (J. Clementson 2010).

- **MonaLisa** was added to NSTX-U in 2016 to provide a total wavelength coverage from 8 – 440 Å with a time-resolution down to 5 ms (M.E. Weller 2016).

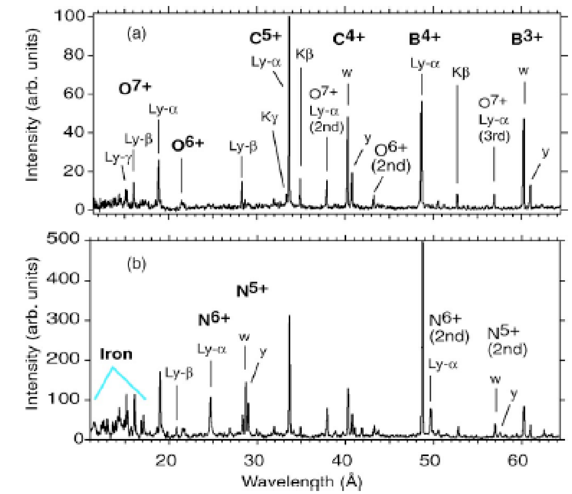

XEUS data from P. Beiersdorfer 2008

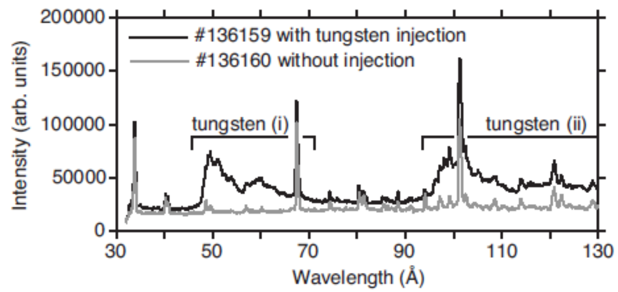

LoWEUS data from J. Clementson 2010

NSTX-U is a Major Advancement from NSTX and Will be a Challenge to PFCs

NSTX (1999 - 2011)

NSTX-U (2015 →)

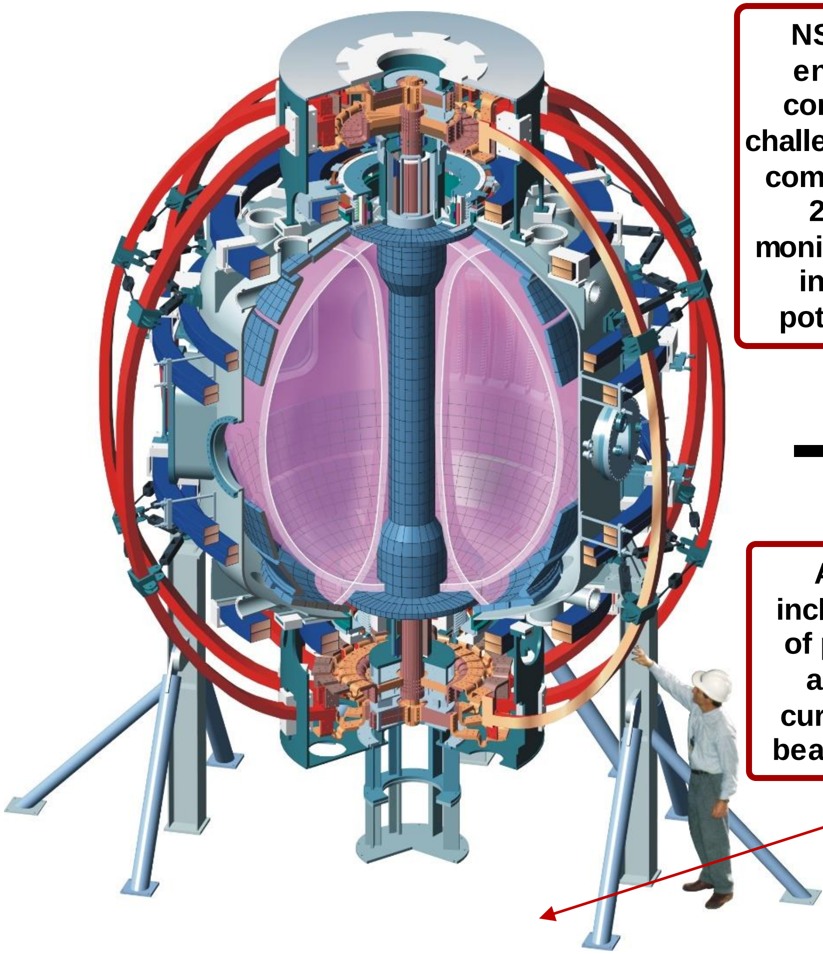

NSTX-U provides enhanced plasma conditions that will challenge plasma facing components (Menard 2012). Impurity monitoring will be vital in catching early potential problems.

Advancements include the doubling of parameters such as toroidal field, current, and neutral beam injector power.

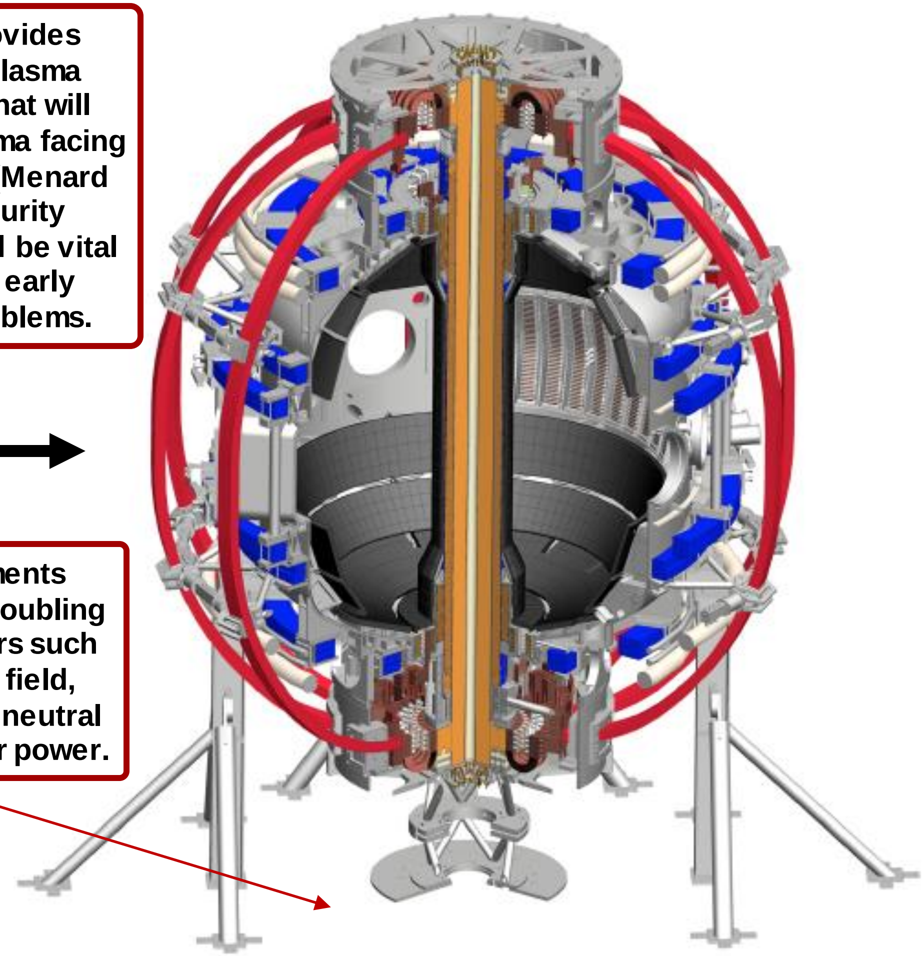

0.5 T, 1 MA, R_0 ~ 0.85 m, A ≥ 1.28, NBI_{max} = 7 MW

1.0 T, 2 MA, R_0 ~ 0.90m, A ≥ 1.5, NBI_{max} = 14 MW

PFCs are Conditioned to Reduce Impurities in the Plasma

- Carbon is the PFC material on NSTX-U in the form of graphite tiles.
  - Low-Z element which minimizes radiative cooling compared to high-Z materials.
- Other impurities on NSTX-U include iron, copper, nickel, titanium, and molybdenum.
  - These metal impurities mainly compose stainless steel and RF antenna.
- Conditioning techniques to reduce sputtering from PFCs include:
  - **Bake out**: Heating the vacuum chamber to ~350 °C to remove water.
  - **Lithium evaporation**: Li has strong chemical affinity to hydrogen and deuterium, thereby suppressing recycling, which reduces impurities.
  - **Glow discharge cleaning**: With D_2 or He, effective in reducing oxygen impurities
    - **Boronization**: glow discharge cleaning with deuterated trimethyl boron.
- EUV spectroscopy detects and monitors impurities.

XEUS, MonaLisa, and LoWEUS Settings and Pictures on NSTX-U

Spectrometer	Wavelength Range (Å)	Hitachi Grating (ℓ/mm)	Focal Distance (cm)	Angle of Incidence (°)	Slit (μm)	FWHM (Å)	Resolution (Å/ΔÅ)
XEUS	5 - 65	2400	23	1.3	100	0.1	50 - 650
MonaLisa	50 – 220	1200	23	3.0	100	0.3	170 - 730
LoWEUS	190 – 440	1200	23	3.0	100	0.3	630 - 1470

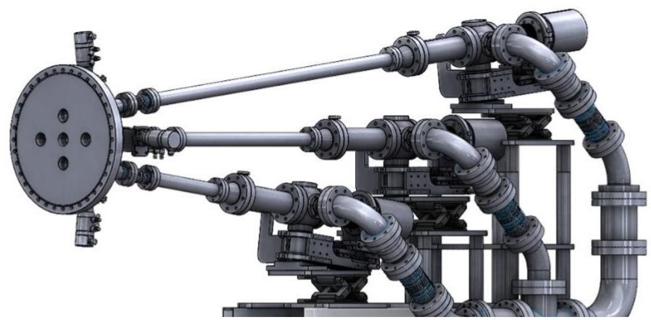

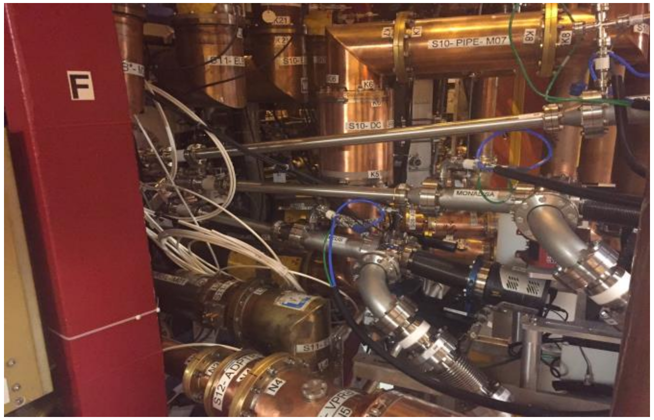

Spectrometers Mounted on NSTX-U

XEUS, MonaLisa, and LoWEUS are flat-field grazing incidence spectrometers (Nakano 1984) which provide high resolution in the EUV range.

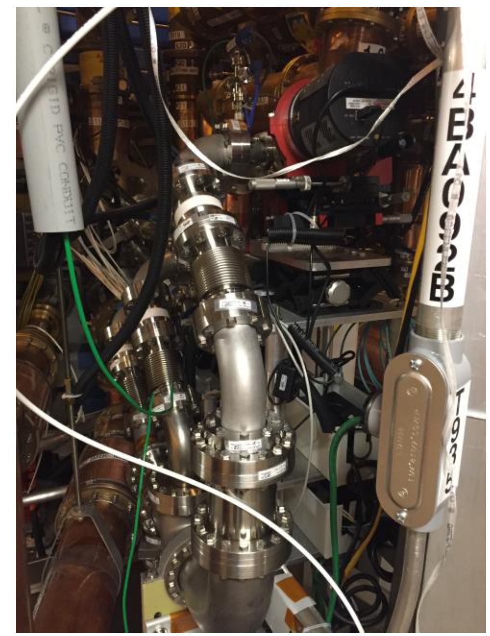

Spectrometers Mounted on NSTX-U

Spectrometer Locations

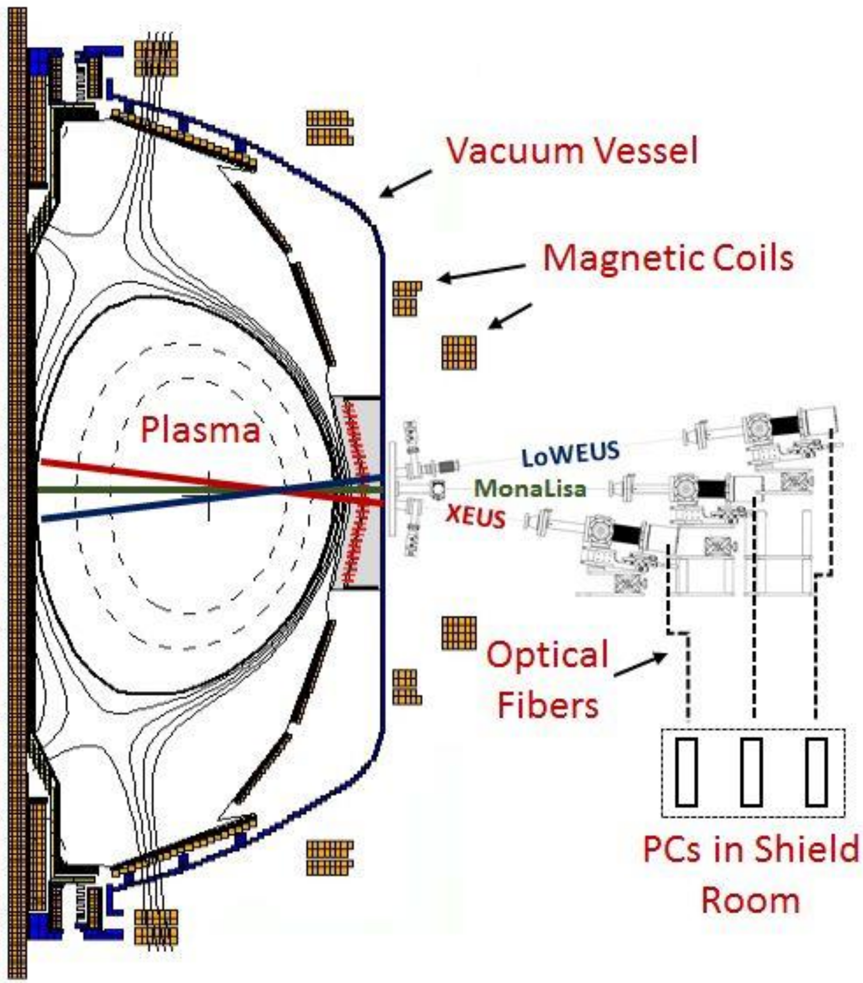

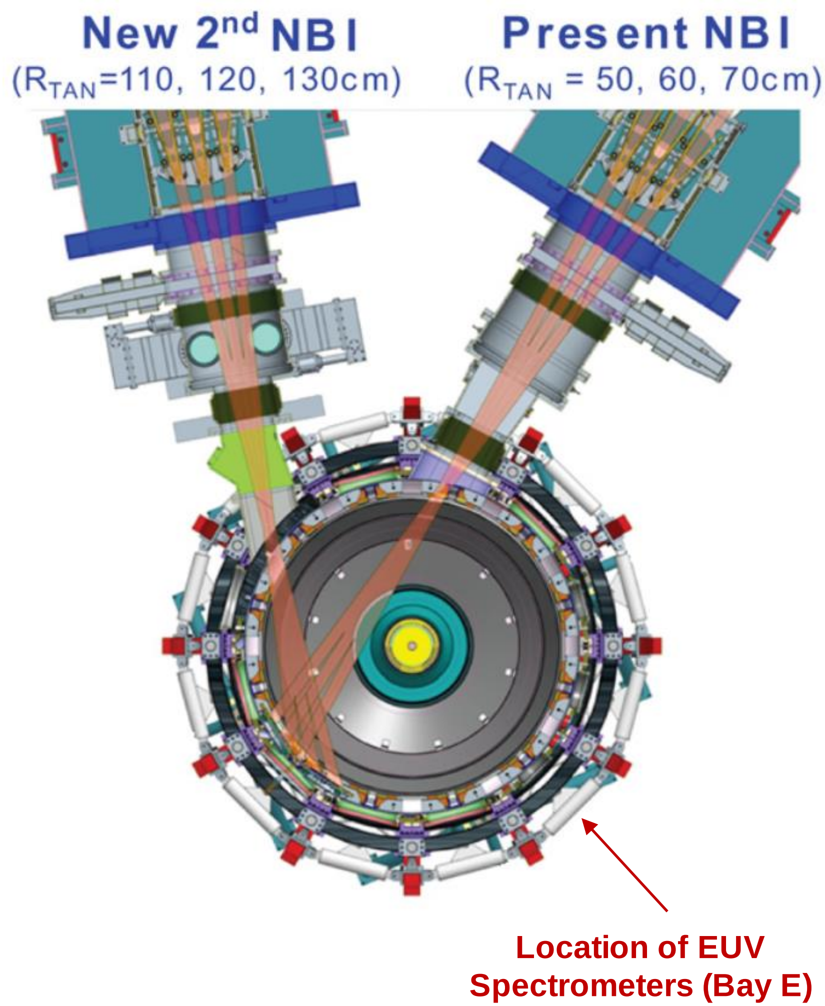

Summary of Data Collected on NSTX-U

- First data collected on May 9th, starting from NSTX-U shot 204563
- Operated during a total of approximately 240 plasma shots over 12 run days
- Total wavelength coverage approximately 8 – 440 Å
  – X-ray and Extreme Ultraviolet Spectrometer (XEUS): 8 – 70 Å, 0.1 Å FWHM
  – Metal Monitor and Lithium Spectrometer Assembly (MonaLisa): 50 – 220 Å, 0.3 Å FWHM (not fully focused yet)
  – Long-Wavelength Extreme Ultraviolet Spectrometer (LoWEUS): 190 – 440 Å, 0.3 Å FWHM
- Temporal Resolution
  – Full Frame (for calibration, good signal to noise): 70 ms
  – Full Bin (for fast readout times, problems with x-ray and neutron noise): 3 – 5 ms
  – Region of Interest (medium readout time, medium signal to noise): 8 – 13 ms
- Confirmed Elements measured on EUV Spectrometers:
  – He, Li, B, C, N, O, Ti, Cr, Fe, and Ni
- Published first data in RSI (M.E. Weller *et al*., RSI **87**, 11E324, 2016)

Example of Experimental Results for XEUS

NSTX-U 205079, 130 - 200 ms

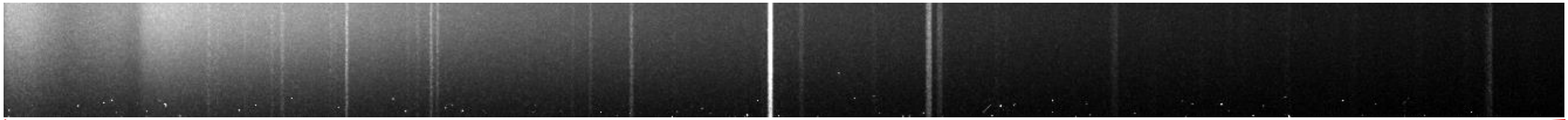

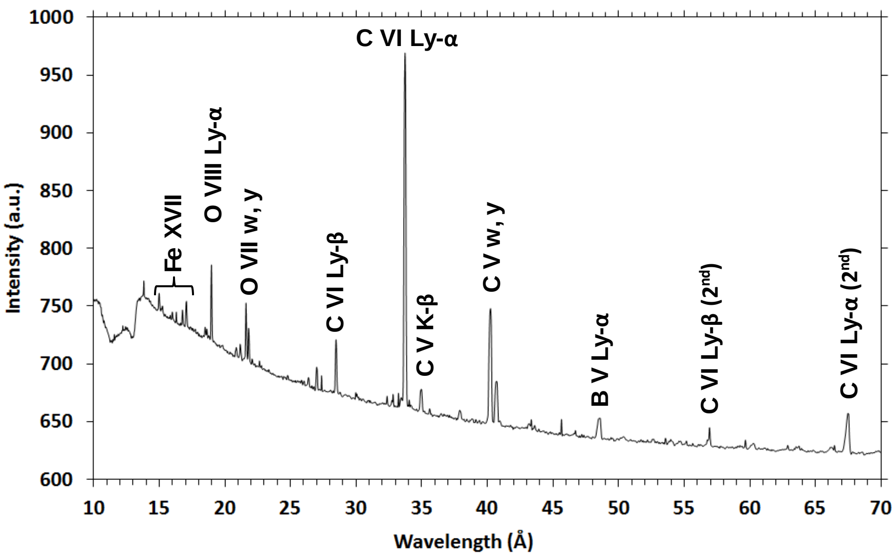

Lines	Transition	λ (Å)
O VIII Ly-α	$2p\ ^2P_{1/2,3/2} \rightarrow 1s\ ^2S_{1/2}$	18.97
O VII ω	$1s2p\ ^1P_1 \rightarrow 1s^2\ ^1S_0$	21.60
O VII y	$1s2p\ ^3P_1 \rightarrow 1s^2\ ^1S_0$	21.80
C VI Ly-β	$3p\ ^2P_{1/2,3/2} \rightarrow 1s\ ^2S_{1/2}$	28.46
C VI Ly-α	$2p\ ^2P_{1/2,3/2} \rightarrow 1s\ ^2S_{1/2}$	33.73
C V ω	$1s2p\ ^1P_1 \rightarrow 1s^2\ ^1S_0$	40.26
C V y	$1s2p\ ^3P_1 \rightarrow 1s^2\ ^1S_0$	40.72
B V Ly-α	$2p\ ^2P_{1/2,3/2} \rightarrow 1s\ ^2S_{1/2}$	48.58
Fe XVII 3C	$2p^53d\ ^1P_1 \rightarrow 2p^6\ ^1S_0$	15.02
Fe XVII 3D	$2p^53d\ ^3D_1 \rightarrow 2p^6\ ^1S_0$	15.28
Fe XVII 3F	$2p^53s\ ^1P_1 \rightarrow 2p^6\ ^1S_0$	16.81
Fe XVII 3G	$2p^53s\ ^3P_1 \rightarrow 2p^6\ ^1S_0$	17.08

C, O, B, and Fe lines identified for first results from XEUS. L-shell Fe lines radiate from various stainless steel components.

Example of Experimental Results on MonaLisa

NSTX-U 205079, 60 - 130 ms

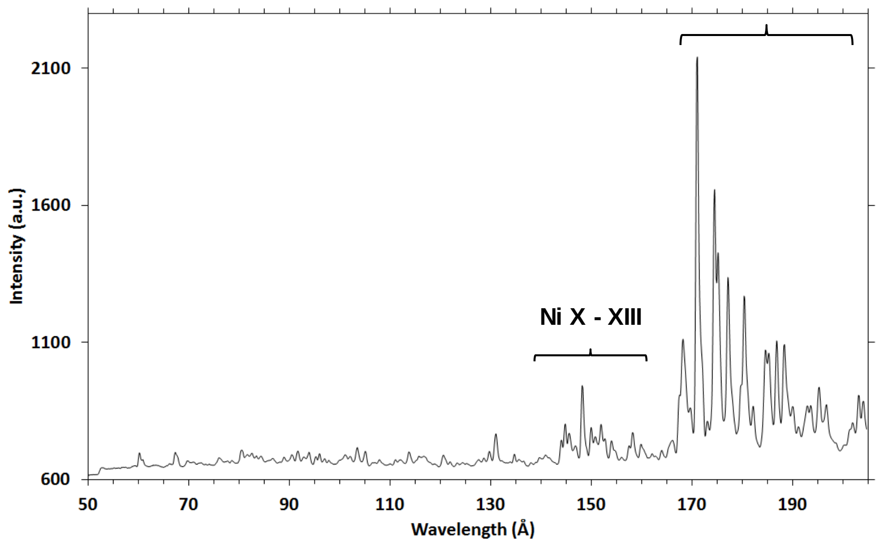

Lines	Transition	λ (Å)
Fe VIII	$3p^5 3d^2\ ^2D_{5/2} \rightarrow 3d\ ^2D_{5/2}$	168.2
Fe IX	$3p^5 3d\ ^1P_1 \rightarrow 3p^6\ ^1S_0$	171.1
Fe X	$3p^4 3d\ ^2D_{5/2} \rightarrow 3p^5\ ^2P_{3/2}$	174.5
Fe X	$3p^4 3d\ ^2P_{3/2} \rightarrow 3p^5\ ^2P_{3/2}$	177.2
Fe X	$3p^4 3d\ ^2P_{1/2} \rightarrow 3p^5\ ^2P_{1/2}$	180.4
Fe X	$3p^4 3d\ ^2S_{1/2} \rightarrow 3p^5\ ^2P_{3/2}$	184.5
Fe XI	$3p^3 3d\ ^3D_3 \rightarrow 3p^4\ ^3P_2$	180.4
Fe XI	$3p^3 3d\ ^3P_2 \rightarrow 3p^4\ ^3P_2$	188.2
Fe XII	$3p^2 3d\ ^2D_{3/2} \rightarrow 3p^3\ ^2P_{1/2}$	188.2
Fe XII	$3p^2 3d\ ^4P_{5/2} \rightarrow 3p^3\ ^4S_{3/2}$	195.1
Fe XIII	$3p3d\ ^1F_3 \rightarrow 3p^2\ ^1D_2$	196.5
Ni XI	$3p^5 3d\ ^1P_1 \rightarrow 3p^6\ ^1S_0$	148.4

During early time on NSTX-U, the spectrum is dominated by M-shell lines of Fe and Ni, which come from stainless steel.

Example of Experimental Results on MonaLisa

NSTX-U 205079, 760 - 830 ms

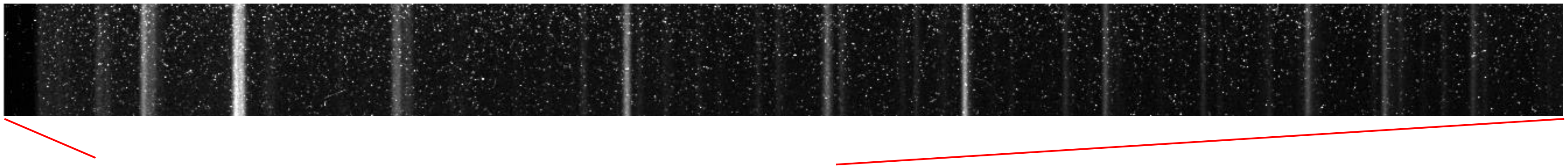

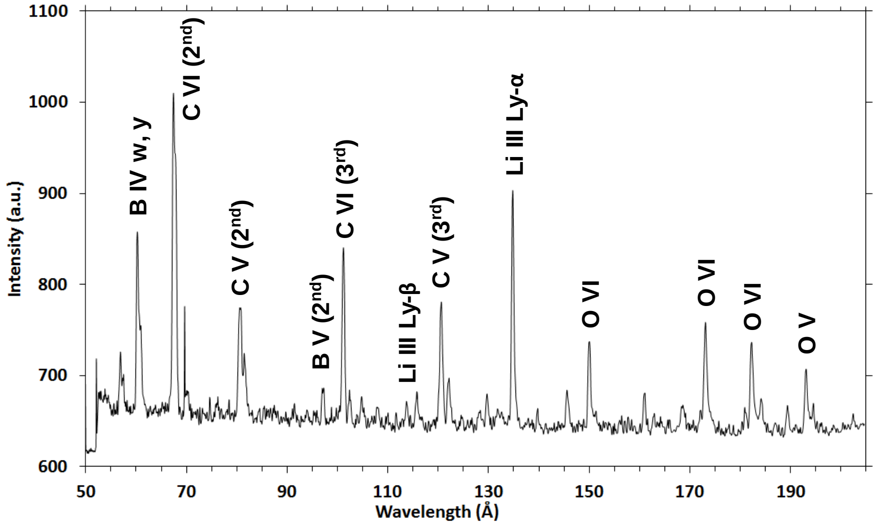

Lines	Transition	λ (Å)
Li III Ly-β	$3p\ ^2P_{1/2,3/2} \rightarrow 1s\ ^2S_{1/2}$	113.9
Li III Ly-α	$2p\ ^2P_{1/2,3/2} \rightarrow 1s\ ^2S_{1/2}$	134.9
O VI	$3p\ ^2P_{1/2,3/2} \rightarrow 2s\ ^2S_{1/2}$	150.1
O VI	$3d\ ^2D_{3/2,5/2} \rightarrow 2p\ ^2P_{1/2,3/2}$	173.1
O VI	$3s\ ^2S_{1/2} \rightarrow 2p\ ^2P_{1/2,3/2}$	184.1
O V	$2s3d\ ^3D_1 \rightarrow 2s2p\ ^3P_1$	192.8

After a few hundred ms, usually after NBI's are turned on, the spectrum is dominated by Li, B, C, and O lines.

Example of Experimental Results on LoWEUS

NSTX-U 205079, 60 - 130 ms

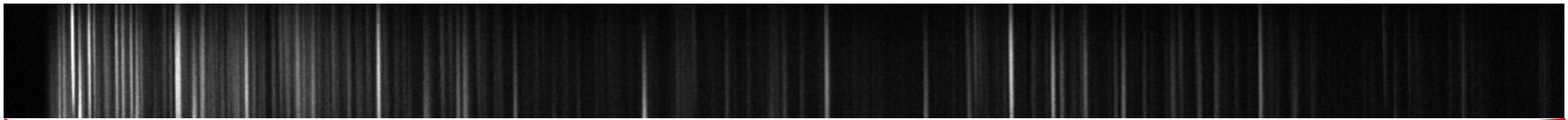

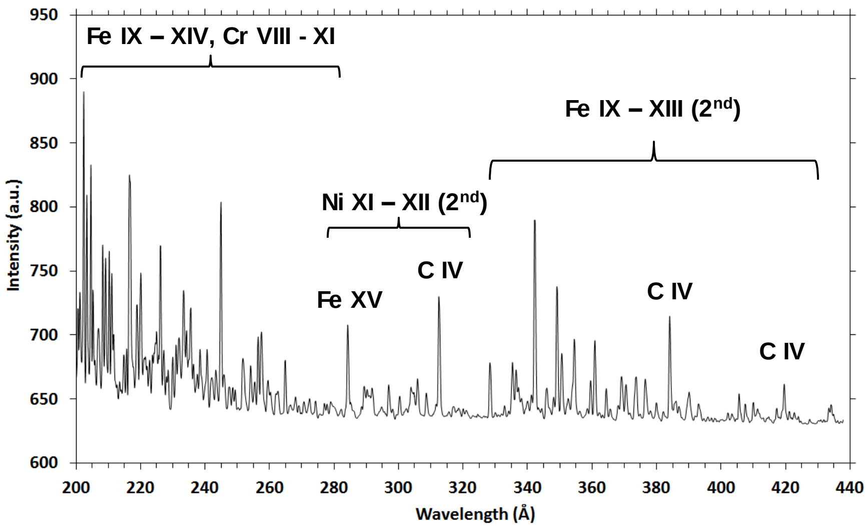

Lines	Transition	λ (Å)
Fe XIII	$3p3d\ ^3D_3 \rightarrow 3p^2\ ^3P_2$	203.8
Fe XIV	$3d\ ^2D_{5/2} \rightarrow 3p\ ^3P_{3/2}$	219.1
Fe XV	$3s3p\ ^1P_1 \rightarrow 3s^2\ ^1S_0$	284.2
Fe XVI	$3p\ ^2P_{3/2} \rightarrow 3s\ ^2S_{1/2}$	335.4
Fe XVI	$3p\ ^2P_{1/2} \rightarrow 3s\ ^2S_{1/2}$	360.8
Ni XVII	$3s3p\ ^1P_1 \rightarrow 3s^2\ ^1S_0$	249.2
Ni XVIII	$3p\ ^2P_{3/2} \rightarrow 3s\ ^2S_{1/2}$	292.0
Ni XVIII	$3p\ ^2P_{1/2} \rightarrow 3s\ ^2S_{1/2}$	320.6
Cr XIII	$3s3p\ ^1P_1 \rightarrow 3s^2\ ^1S_0$	328.3
Cr XIV	$3p\ ^2P_{3/2} \rightarrow 3s\ ^2S_{1/2}$	389.9
Cr XIV	$3p\ ^2P_{1/2} \rightarrow 3s\ ^2S_{1/2}$	412.1

During early time on NSTX-U, the spectrum is dominated by M-shell lines of Fe, Ni, and Cr, followed by C.

Example of Experimental Results on LoWEUS

NSTX-U 205079, 760 - 830 ms

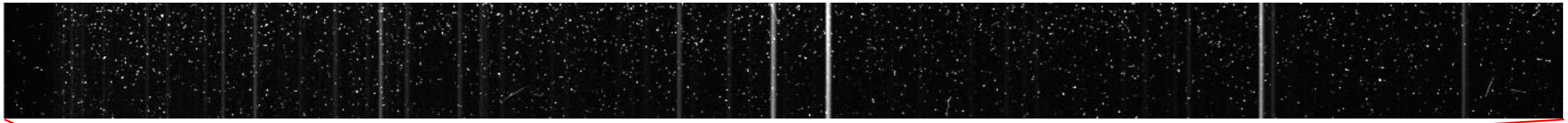

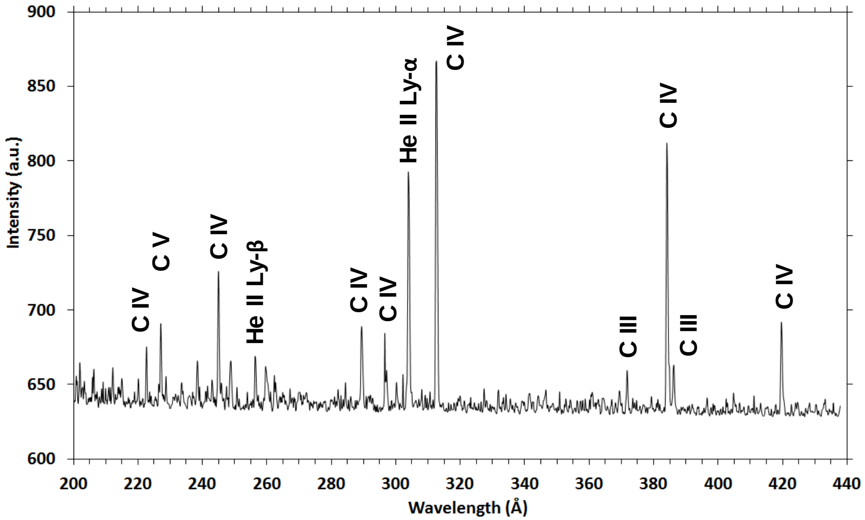

After a few hundred ms, usually after NBI's are turned on, the spectrum is dominated by He, C, and O lines.

Lines	Transition	λ (Å)
He II Ly-β	$3p\ ^2P_{1/2,3/2} \rightarrow 1s\ ^2S_{1/2}$	256.3
He II Ly-α	$2p\ ^2P_{1/2,3/2} \rightarrow 1s\ ^2S_{1/2}$	303.8
C IV	$5p\ ^2P_{3/2} \rightarrow 2s\ ^2S_{1/2}$	222.8
C IV	$4p\ ^2P_{3/2} \rightarrow 2s\ ^2S_{1/2}$	244.9
C IV	$4d\ ^2D_{5/2} \rightarrow 2p\ ^2P_{3/2}$	289.2
C IV	$3p\ ^2P_{3/2} \rightarrow 2s\ ^2S_{1/2}$	312.4
C IV	$3d\ ^2D_{5/2} \rightarrow 2p\ ^2P_{3/2}$	384.2
C IV	$3s\ ^2S_{1/2} \rightarrow 2p\ ^2P_{3/2}$	419.7
C V	$3p\ ^3P_2 \rightarrow 2s\ ^3S_1$	227.2

Evolution of Spectra in LoWEUS

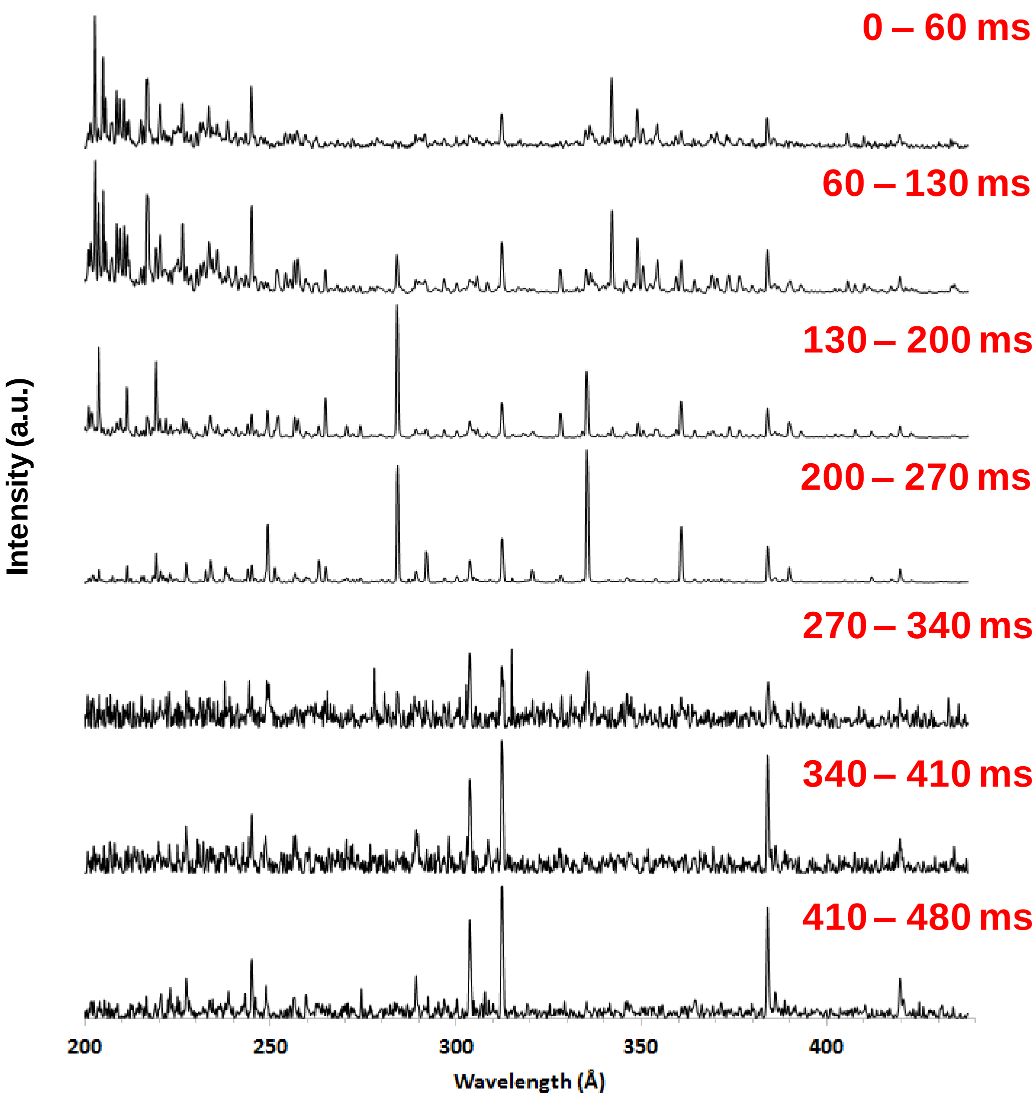

- First frame shows Fe VII – XII, Cr VI – XII, Ni IX – XIV, and C IV.
- Second frame shows plasma heating up, ionizing into Fe XV and Cr XIII.
- By third frame most lower ionizing stage of Fe, Cr, and Ni are gone, and Fe XV – XVI, Cr XIII – XIV, and Ni XVII – XVIII are dominant features.
- Fourth frame hotter still, with clear He and C lines mixed with Fe, Cr, and Ni.
- Radical change in spectra as NBI turned on, increasing noise, and SS components practically disappear.
- For the most part only He II and C IV lines are seen as the plasma enters flattop phase.
- After 400 ms the plasma is well controlled and mostly He, C, and a few O lines are seen.

Evolution of Spectra in LoWEUS (2)

- **Fast forward toward past 700 ms, He and C lines still dominate.**
- **After 970 ms, M-shell lines of Ti VI - IX appear.**
- **Ti heats up in the plasma. C and He still present.**
- **After 1110 the plasma is ramping down. O and Li lines increase in intensity and N appears, likely emitting from boron nitride.**

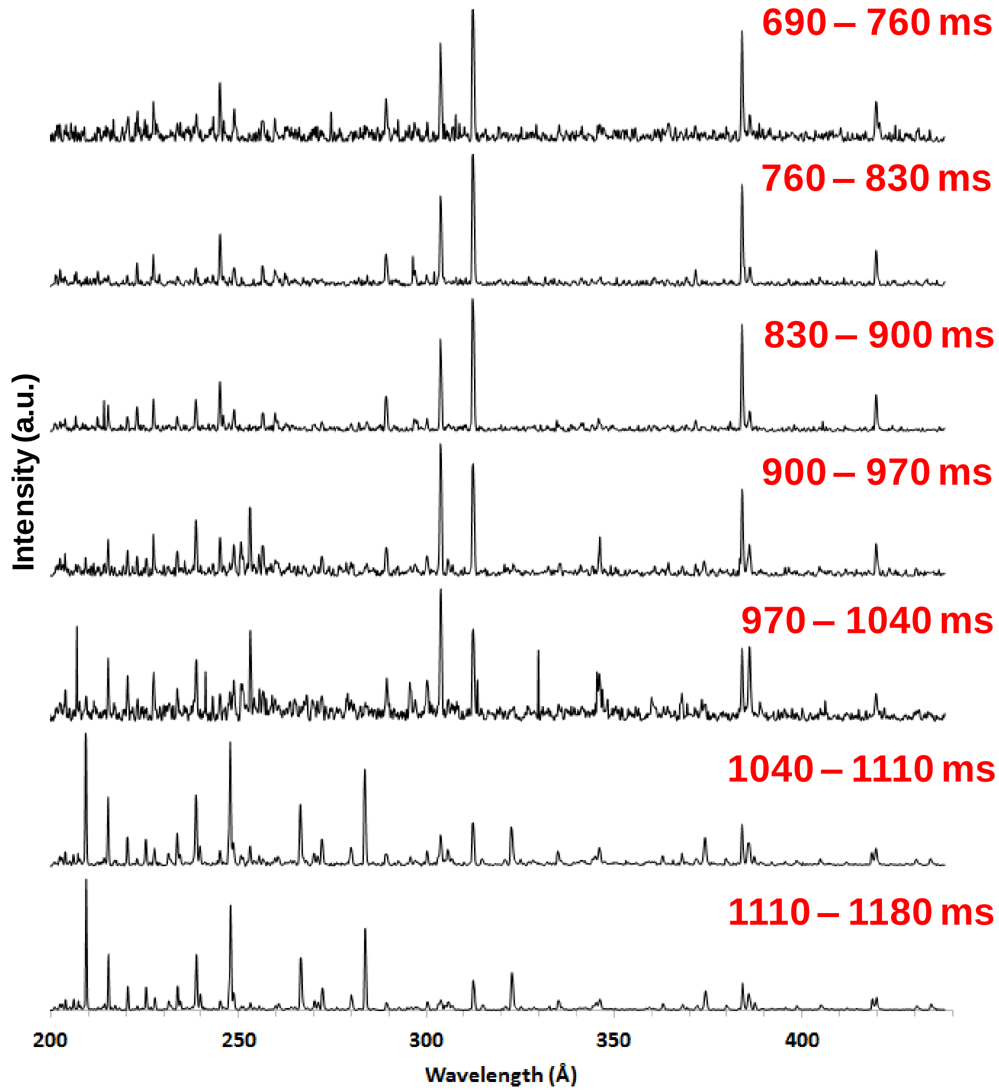

Lines Identified in LoWEUS

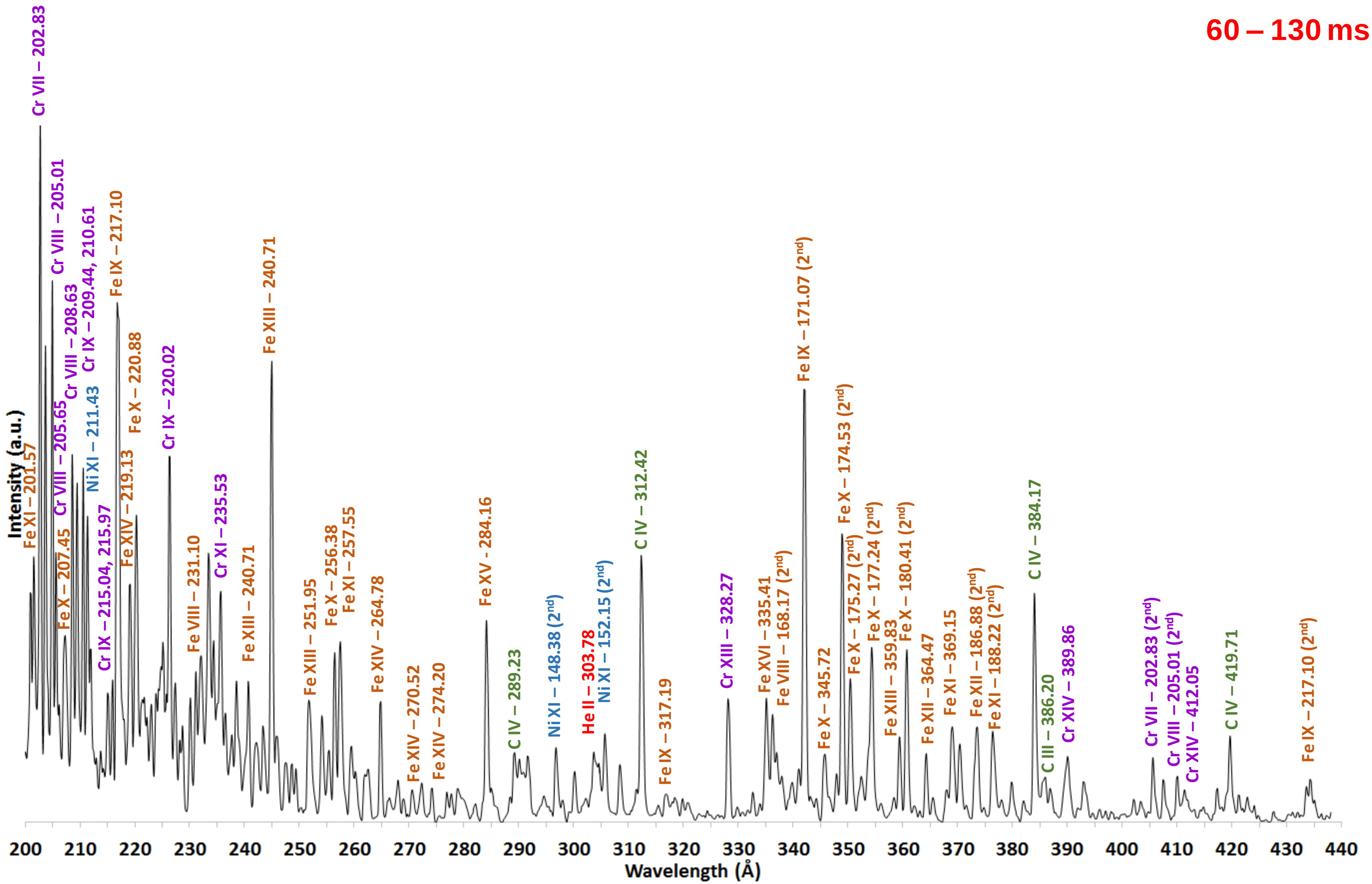

Lines Identified in LoWEUS

200 – 270 ms

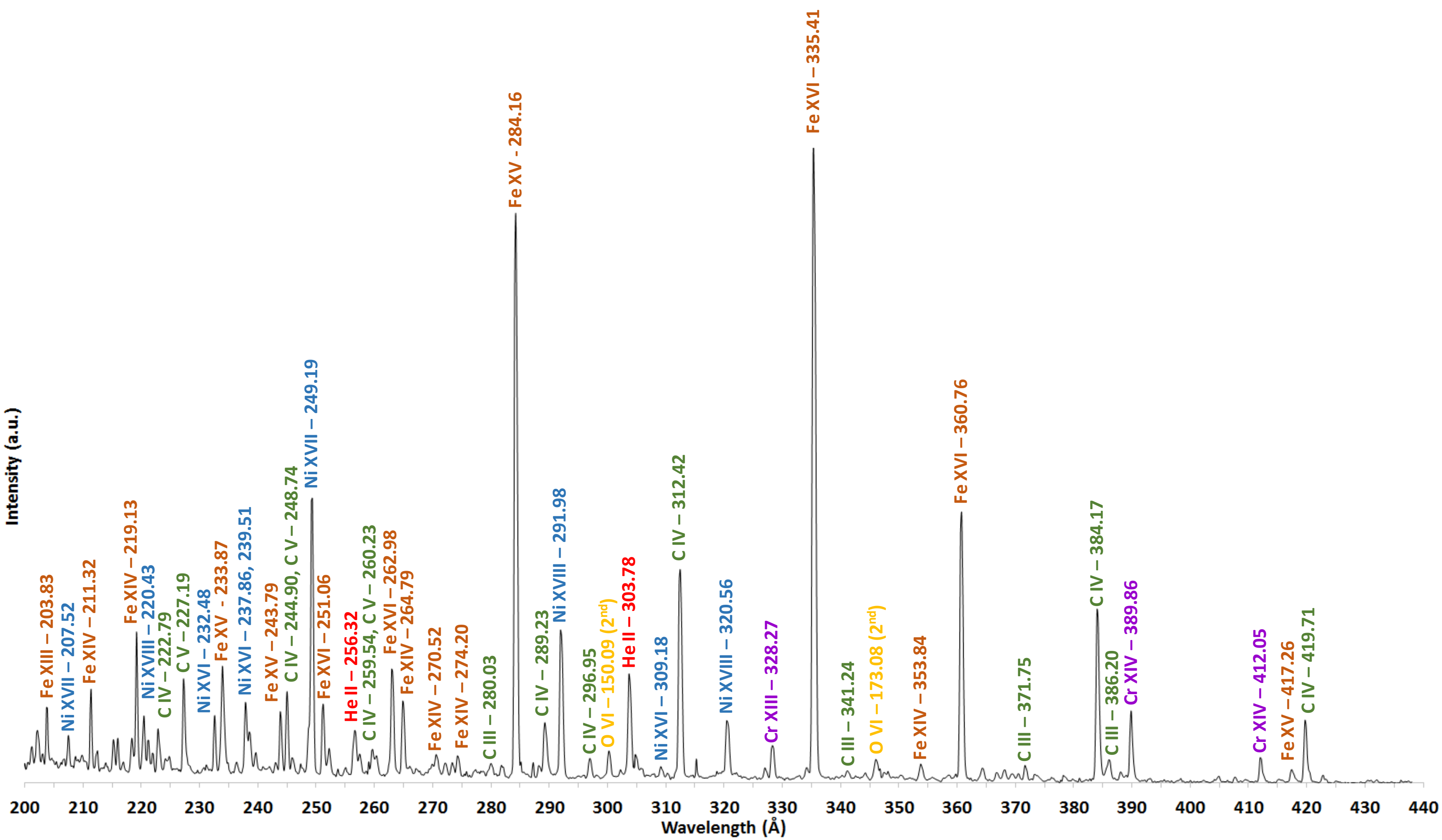

Lines Identified in LoWEUS

970 – 1040 ms

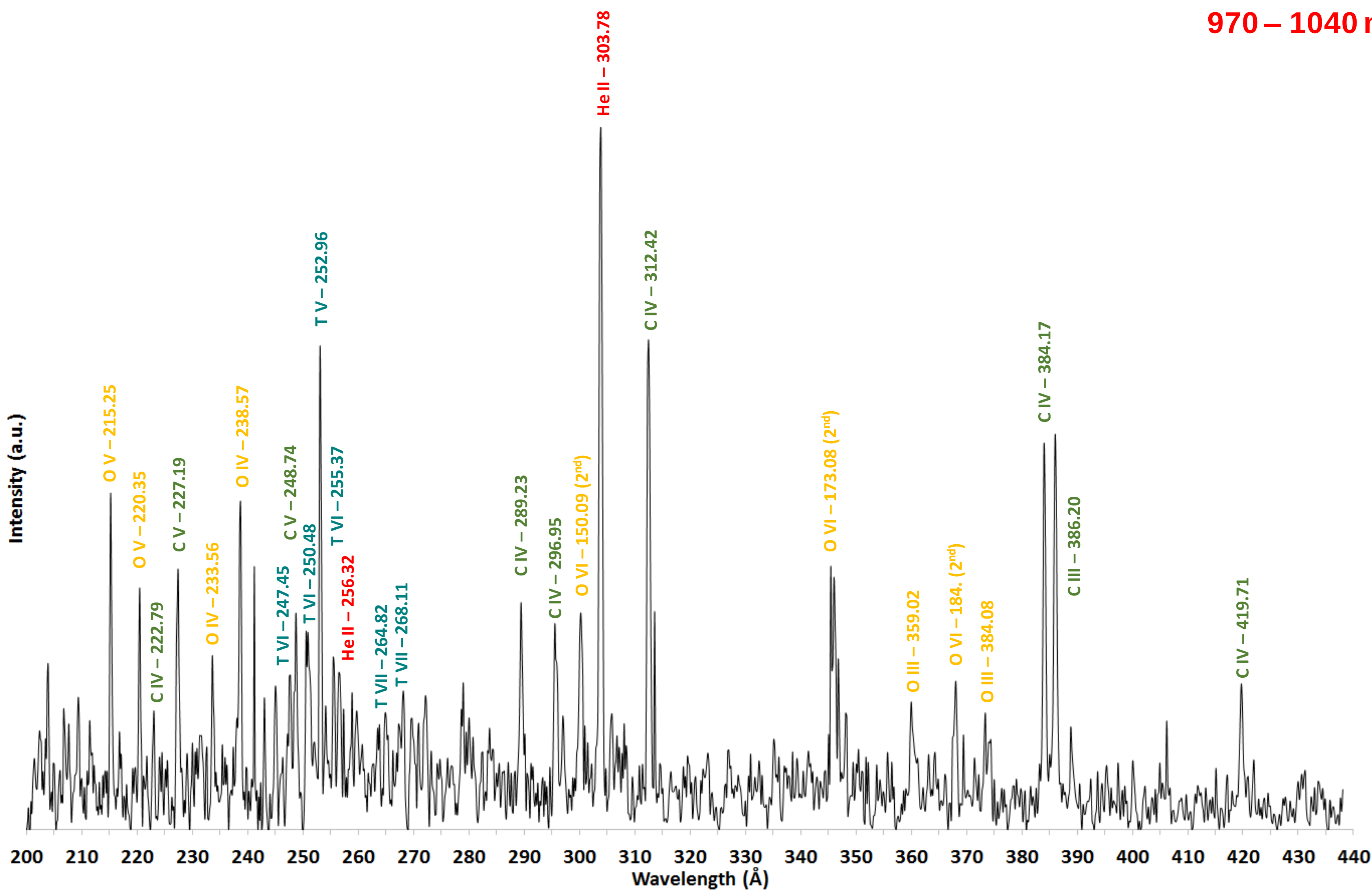

Lines Identified in LoWEUS

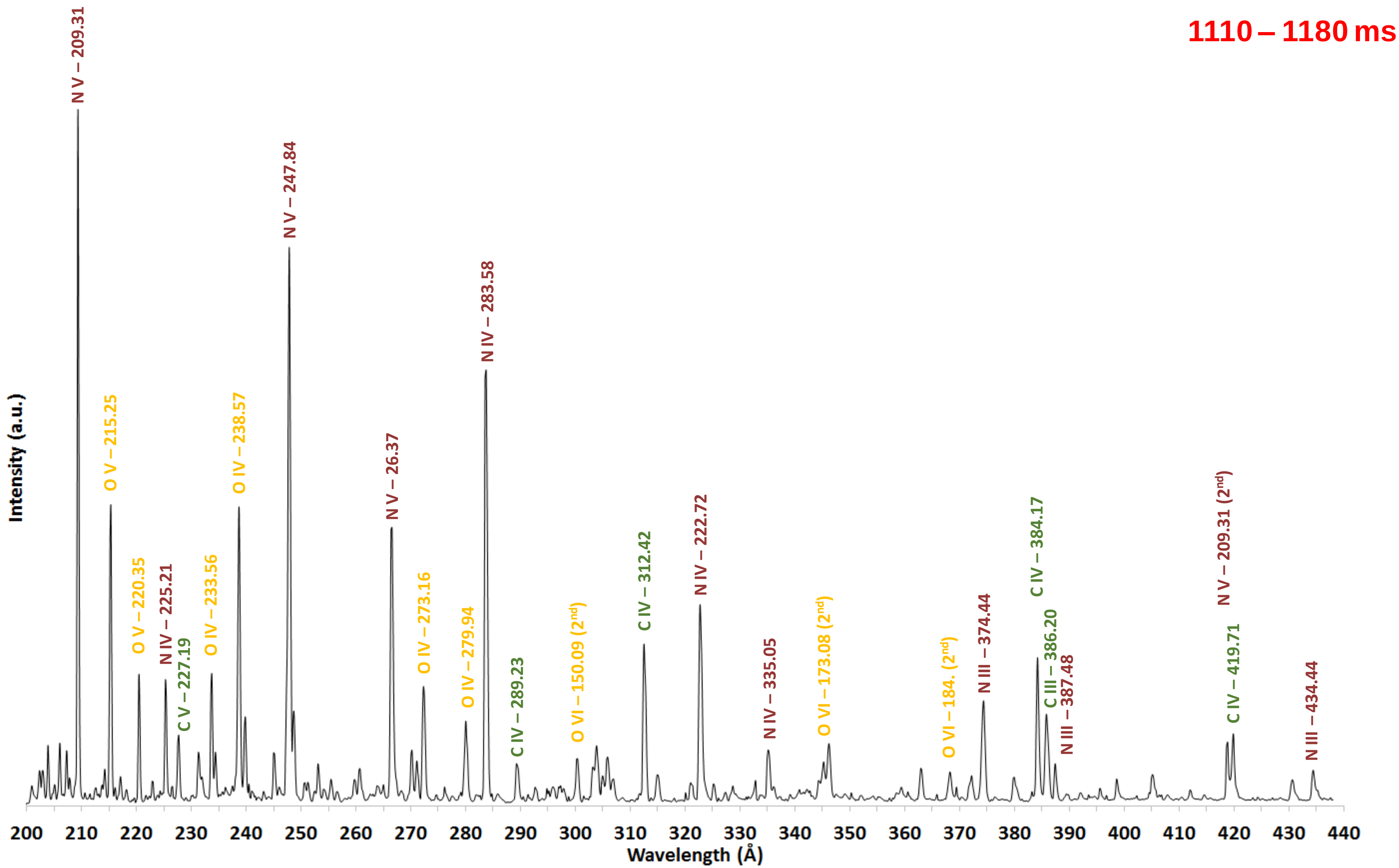

Where Does Ti Emission Come From?

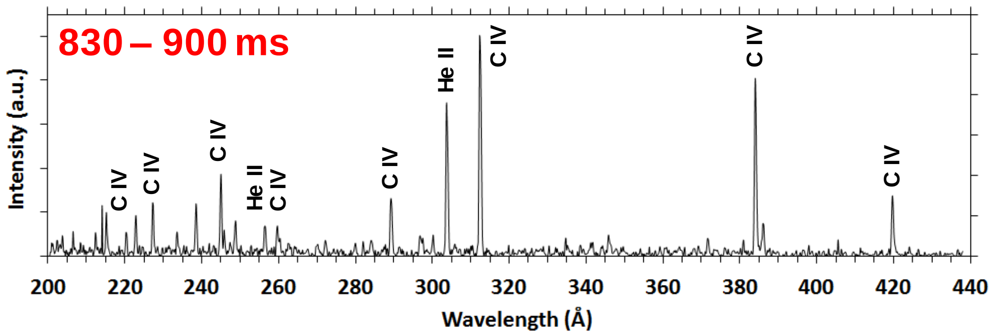

Ti likely emits from Ti carbide that coats the Faraday shield of the HHFW antenna. To the right are magnetic equilibrium reconstruction right before and after Ti appears, along with plasma tv* images showing the glow from the shielding.

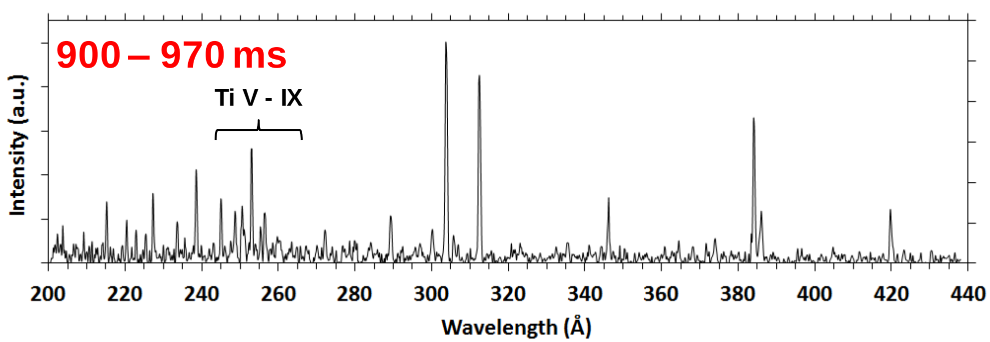

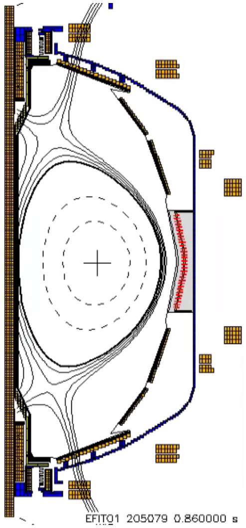

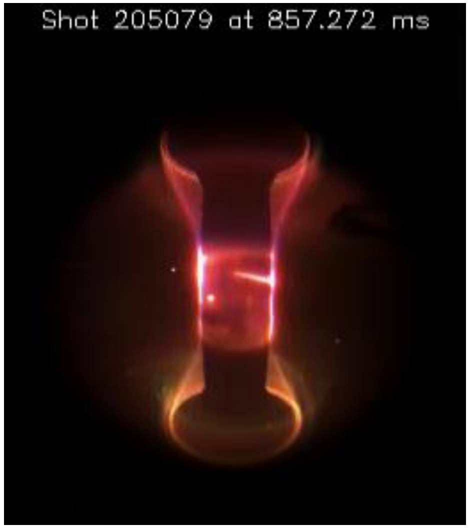

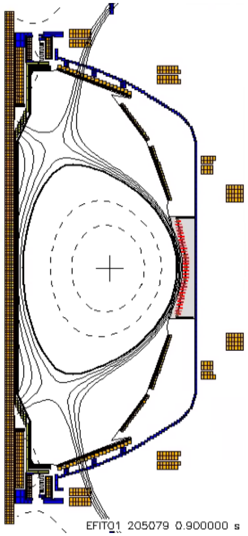

*Credit M.A. Jaworski

Where Does N Emission Come From?

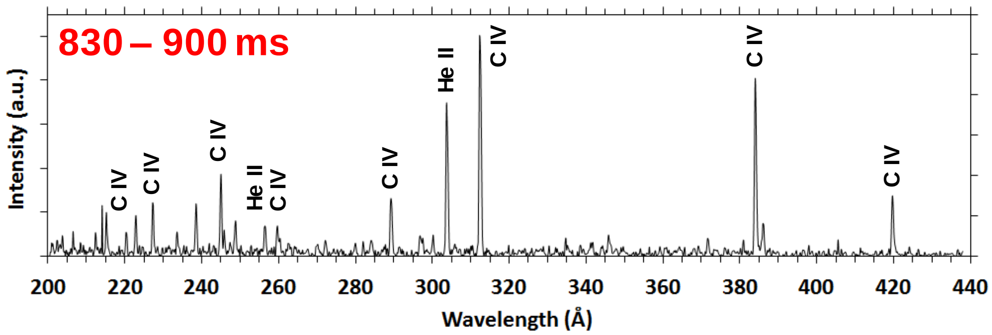

N likely emits from boron nitride limiter. To the right are magnetic equilibrium reconstruction before and then after N appears, along with plasma tv* images showing the glow from the shielding. B, O, and Li also increase in intensity when N appears.

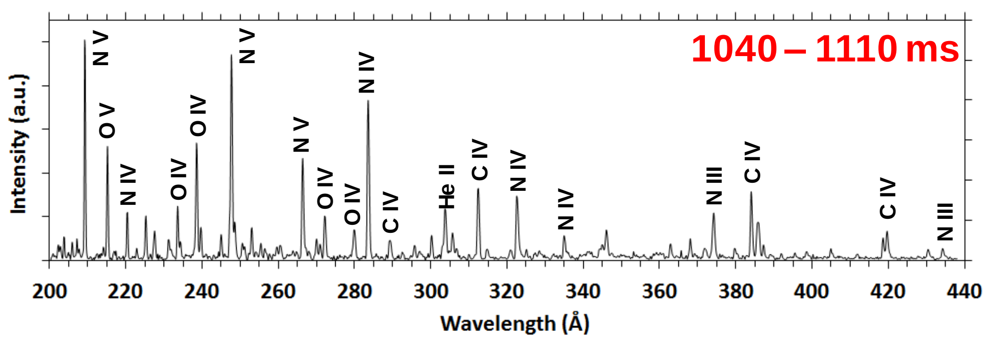

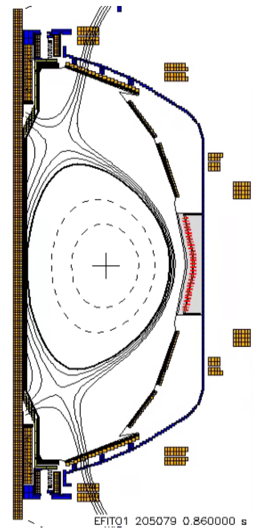

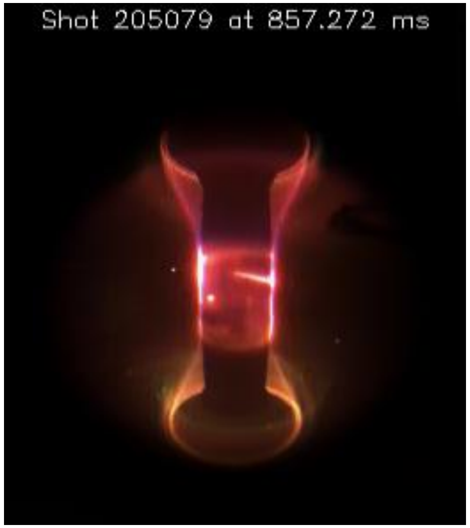

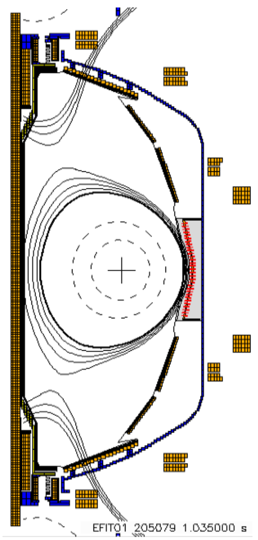

*Credit M.A. Jaworski

Line Histories of 205079

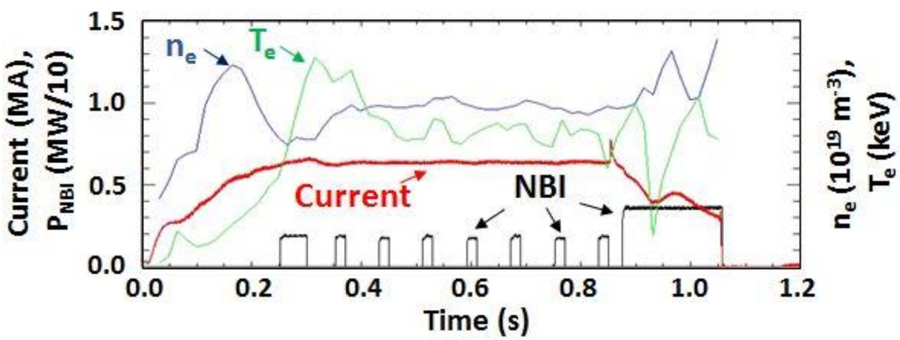

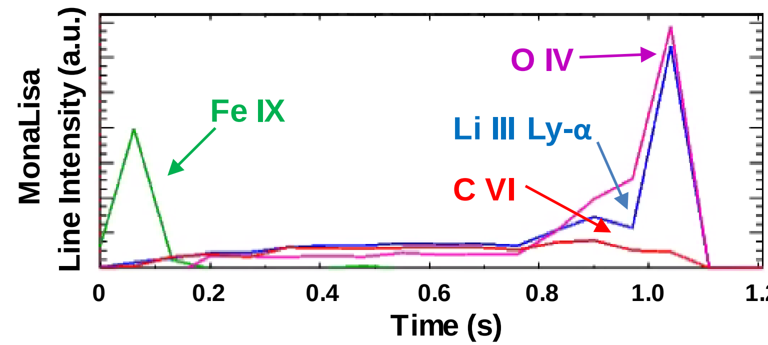

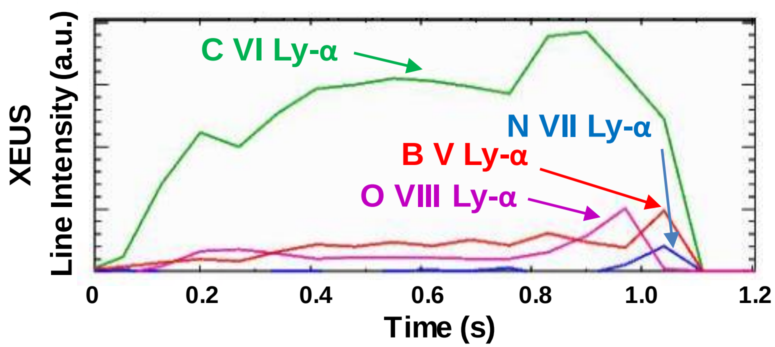

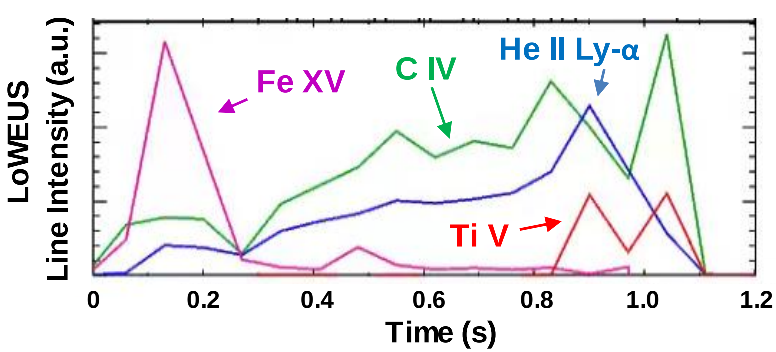

Signals of current, NBI power, and electron density and temperature (Thompson scattering) are plotted along with line intensity profiles of diagnostically important lines from XEUS, LoWEUS, and MonaLisa.

Fe (from SS components) radiate early while Ti and N radiate very late. C, He, O, B, and Li are all present throughout much of the experiment, with C being the dominant feature.

These line profiles can be used to assess wall conditions and to diagnose potential problems.

Relative Calibration of LoWEUS

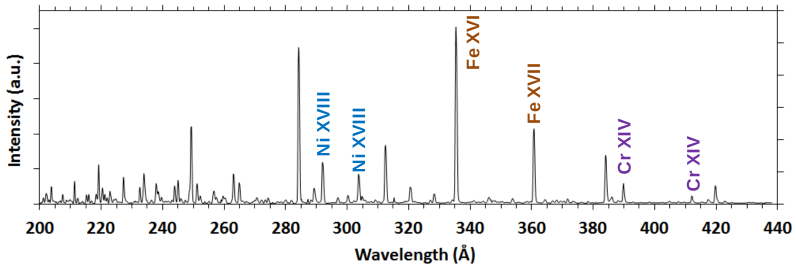

Lines	Transition	λ (Å)	Theory Ratio*
Ni XVIII	3p $^2P_{3/2,1/2}$ → 3s $^2S_{1/2}$	292.0/320.6	1.94
Fe XVI	3p $^2P_{3/2,1/2}$ → 3s $^2S_{1/2}$	335.4/360.8	1.95
Cr XIV	3p $^2P_{3/2,1/2}$ → 3s $^2S_{1/2}$	389.9/412.1	1.96

The Na-like doublets of Ni XVIII, Fe XVI, and Cr XIV are insensitive to n_e and weakly sensitive to T_e (Lawson 2009) and can be used to help with calibration. We then used CHIANTI (Landi 2013) to calculate line intensities of C IV lines using different n_e and T_e normalized to the C IV line at 312.4 Å, similar to Ref (Lepson 2016).

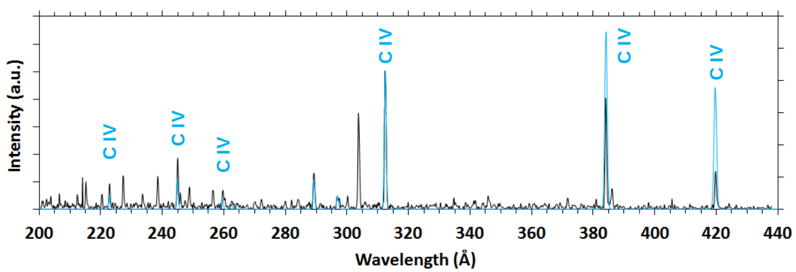

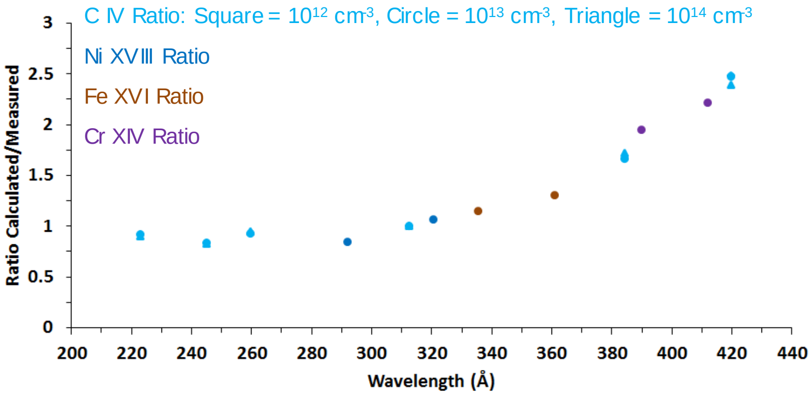

The line ratios of calculated divided by measured are shown above and the responsivity curve, which was best fit by a third order polynomial, is shown below, which can be used to give relative calibration for LoWEUS for most of the spectral range.

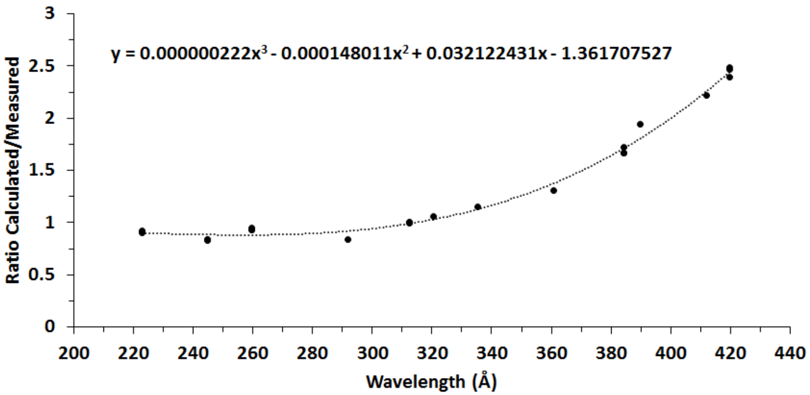

Conclusions

- NSTX-U results of EUV spectra covering the spectral range of 8-440 Å have been shown for the first time
  - Over 240 plasma shots covering 12 run days
- Hundreds of lines identified with confirmed elements:
  - He, Li, B, C, N, O, Ti, Cr, Fe, Ni
- In particular data from LoWEUS covered the spectral range > 250 Å, identifying many new lines on NSTX-U to study
- Radiation dominated by M-shell Fe, Ni, and Cr lines and then dominated by C, followed by He, Li, O, and B
- Occasionally Ti and N appear which correlates with plasma hitting the outer edge
- Calibrated LoWEUS spectrometer to give relative intensities

References

- P. Beiersdorfer *et al*., RSI **77**, 10F306, (2006)
- P. Beiersdorfer *et al*., RSI **79**, 10E318, (2008)
- J. Clementson *et al*., J. Phys. B **43**, 144009 (2010)
- J. Clementson *et al*., RSI **81**, 10E326, (2010)
- J.K. Lepson *et al*., J. Phys. B: A. Mol. Opt. Phys. **43**, 114018 (2010)
- J.K. Lepson *et al*., J. Phys: Con. Ser. **583**, 012012 (2015)
- J.E. Menard *et al*., Nucl. Fusion **52**, 083015, (2012)
- N. Nakano *et al*., Applied Optics **23**, 2386, (1984)
- A.M. Niles *et al*., RSI **77**, 10F106, (2006)
- M.E. Weller *et al*., PoP **21**, 031206, (2014)
- M.E. Weller *et al*., RSI **87**, 11E324, (2016)
- J.K. Lepson *et al*., RSI **87**, 11D614, (2016)
- E. Landi *et al*., Astro. J., **86**, 763 (2013)
- K.D. Lawson *et al*., EFDA–JET–R(09)01